Simultaneous reduction of iron–sulfur protein and cytochrome b_L during ubiquinol oxidation in cytochrome bc_1 complex

Jian Zhu*†, Tsuyoshi Egawa‡, Syun-Ru Yeh‡, Linda Yu*, and Chang-An Yu*§

*Department of Biochemistry and Molecular Biology, Oklahoma State University, Stillwater, OK 74078; and ‡Department of Physiology and Biophysics, Albert Einstein College of Medicine of Yeshiva University, Bronx, NY 10461

Edited by Helmut Beinert, University of Wisconsin, Madison, WI, and approved January 30, 2007 (received for review September 6, 2006)

The key step of the protonmotive Q-cycle mechanism of the cytochrome bc_1 complex is the bifurcated oxidation of ubiquinol at the Qp site. It was postulated that the iron–sulfur protein (ISP) accepts the first electron from ubiquinol to generate ubisemiquinone anion to reduce b_L. Because of the difficulty of following the reduction of ISP optically, direct evidence for the early involvement of ISP in ubiquinol oxidation is not available. Using the ultra-fast microfluidic mixer and the freeze-quenching device, coupled with EPR, we have been able to determine the presteady-state kinetics of ISP and cytochrome b_L reduction by ubiquinol. The first-phase reduction of ISP starts as early as 100 μs with a $t_{1/2}$ of 250 μs. A similar reduction kinetic is also observed for cytochrome b_L, indicating a simultaneous reduction of both ISP and b_L. These results are consistent with the fact that no ubisemiquinone was detected at the Qp site during oxidation of ubiquinol. Under the same conditions, by using stopped flow, the reduction rates of cytochromes b_H and c_1 were 403 s^{-1} ($t_{1/2}$ 1.7 ms) and 164 s^{-1} ($t_{1/2}$ 4.2 ms), respectively.

EPR | rapid freeze-quenching | stopped-flow | ubiquinol-cytochrome *c* reductase | electron transfer

The cytochrome bc_1 complex (also known as ubiquinol-cytochrome *c* reductase or complex III) is an essential segment of the electron transfer chain of mitochondria and many respiratory and photosynthetic bacteria (1). It catalyzes electron transfer from ubiquinol to cytochrome *c* with concomitant translocation of protons across the membrane to generate a proton gradient and membrane potential for ATP synthesis. The complex from bovine heart mitochondria is composed of 11 protein subunits: three core subunits, subunits III, IV, and V, which house *b*-type cytochromes, *c*-type cytochrome, and iron-sulfur center, respectively, and eight supernumerary subunits that contain no redox prosthetic groups. Cytochrome bc_1 complexes from other sources contain the three major subunits with one to seven supernumerary subunits (2). In either case, the complex contains four redox prosthetic groups: cytochrome b_L (b_{566}) and b_H (b_{562}), cytochrome c_1, and a high potential iron–sulfur cluster (ISC; 2Fe-2S Rieske center).

The 3D structure of the cytochrome bc_1 complexes from beef (3, 4), chicken (5), yeast (6), and *Rhodobacter capusulata* (7) were recently determined. The complex is crystallized in an intertwined dimer form. The iron–sulfur proteins (ISPs) in the two bc_1 monomers are intertwined with the head domain in one monomer interacting with cytochrome *b* and cytochrome c_1 of the other monomer. The intertwined dimer observed in the crystalline complex also exists in solution, which was confirmed (8) in the *R. sphaeroides* bc_1 complex through the formation of a four-subunit (two ISPs and two cytochrome *b*s) adduct by two intersubunit disulfide bonds between two engineered cysteine pairs: one pair links the ISP head domain to cytochrome *b*, and the other pair links the ISP tail domain to cytochrome *b* of another monomer. Two apparently noncommunicating cavities in the dimeric complex are presented: each connecting the Qp pocket of one monomer to the Qn pocket of the other. The distance between the Fe atoms of the two hemes b_L is only 21 Å, which is approximately the same as the distance between heme b_L and b_H in one monomer (Fig. 1). The short distance between the two hemes b_L and the presence of several aromatic amino acid residues at the interface of the two cytochrome *b* proteins have caused investigators (9–12) to speculate about the existence of electron transfer and equilibration between the two hemes b_L. The involvement of an aromatic residue in such an electron transfer has recently been confirmed in the bacterial complex (12).

On the basis of functional data (13, 14) and structural information (3–7), the "protonmotive Q cycle" is the most favored mechanism for electron and proton transfer in the cytochrome bc_1 complex (15, 16). The key step of the Q-cycle mechanism (Fig. 2) is the bifurcation of electrons from ubiquinol at the Qp site. It was postulated that the first electron of ubiquinol is transferred to the "high-potential chain," consisting of the ISP and cytochrome c_1. Then the second electron of ubiquinol is passed through the "low-potential chain" consisting of cytochromes b_L and b_H to reduce ubiquinone or ubisemiquinone bound at the Qn site. Although crystallographic data clearly indicates the presence of two separated quinone binding domains: one for ubiquinol oxidation (Qp) and the other for quinone reduction (Qn), only the binding of ubiquinone (17–19) and the presence of ubisemiquinone radical (20–22) at the Qn site were demonstrated. The binding of ubiquinol or ubiquinone at the Qp site has not been detected even though the binding of various Qp site inhibitors (18, 23, 24) is well known.

The mechanism of the bifurcated oxidation at the Qp site is still a matter of controversy. Evidences supporting "sequential oxidation" (25–28) and the "concerted oxidation" (29–33) of the cytochrome *b*-bound ubiquinol are both available. In the sequential oxidation, the first electron of the ubiquinol is transferred to the ISC, and the resulting ubisemiquinone is used to reduce cytochrome b_L. The absence of detectable ubisemiquinone radical at the Qp site (33) questions the validity of the sequential oxidation mechanism, even though several plausible explanations for the absence of Q-radical have been offered (27, 34). Even though the rate constant for the presteady-state reduction of the cytochrome *b* by ubiquinol is much larger than that of cytochrome c_1, many investigators (35–38) assume that the first electron goes to the ISC, the thermodynamically favorable acceptor. The requirement for ISP (39) during the reduction of cytochrome c_1 by ubiquinol in the

Author contributions: J.Z., T.E., S.-R.Y., L.Y., and C.-A.Y. designed research; J.Z. and T.E. performed research; J.Z., T.E., S.-R.Y., L.Y., and C.-A.Y. analyzed data; and C.-A.Y. wrote the paper.

The authors declare no conflict of interest.

This article is a PNAS direct submission.

Abbreviations: ISP, iron–sulfur protein; ISC, iron–sulfur cluster; DM, dodecyl maltoside; OG, octyl glucoside.

†Present address: Physical Biosciences Division, Lawrence Berkeley National Laboratory, Berkeley, CA 94720.

§To whom correspondence should be addressed. E-mail: cayuq@okstate.edu.

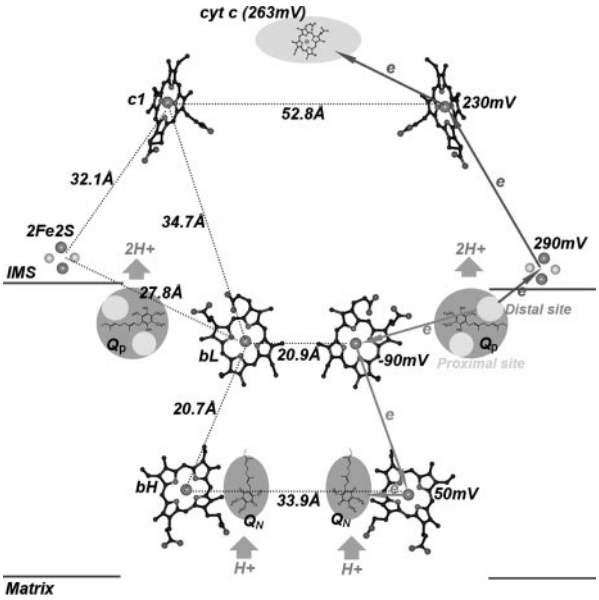

Fig. 1. The relative location of the essential redox groups of the bovine heart mitochondrial cytochrome bc_1 complex (59). The b_L, b_H, and c_1 hemes are shown as ball-and-stick models, whereas the *2Fe2S* clusters are shown as ball models. The quinone oxidation pockets are near the intermembrane space (IMS) side of the membrane, and the quinol reduction pockets are near the matrix side of the membrane. Cytochrome *c* is shown as a shaded oval as labeled. Distances between redox centers are given on the left, and the redox potential for each center is given on the right. The high potential ET path is depicted by arrowed lines pointing upward, and the low potential ET path is shown by arrowed lines pointing downward. Circles in the upper and lower parts within the Qp pockets are distal and proximal quinone bindings, respectively.

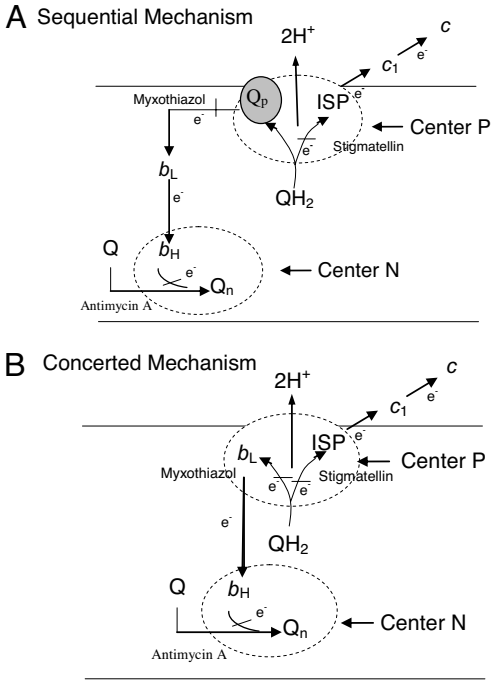

Fig. 2. The proton motive Q-cycle mechanism. (*A*) Sequential bifurcated oxidation of quinol at the Qp site. Ubiquinol bound in cytochrome *b* is first oxidized by ISP to generate an ubisemiquinone radical to reduce cytochrome b_L. (*B*) Concerted bifurcated oxidation of ubiquinol at the Qp site. Bifurcated oxidation of ubiquinol at the Qp site by ISP and cytochrome b_L takes place simultaneously with no generation of ubisemiquinone radical at the Qp site.

cytochrome bc_1 complex supports this assumption. The observed smaller rate constant of cytochrome c_1 reduction, compared with the cytochrome *b* reduction rate constant, was attributed to the slow electron transfer between the ISC and heme c_1. In fact, there is no evidence, so far, showing that the ISC receives an electron from ubiquinol before other redox components, because of the difficulty in detecting the redox change of the ISC in a fast time scale.

Taking advantage of the unique EPR signatures of the ISC (40), cytochromes b_L, b_H, and c_1 (41–43), and ubisemiquinone radical (21, 22), we recently investigated the presteady-state kinetics of ISP and cytochrome b_L reduction by ubiquinol at the Qp site by using an ultra-fast freeze-quenching technique (44) coupled with EPR spectroscopy. Our results are consistent with the concerted oxidation mechanism (29–32) of the ubiquinol at the Qp site, although we could not fully exclude the sequential mechanism because of our limited time resolution of $\approx$50 μs. To further confirm this mechanism, measurements with a better time resolution are required.

Results and Discussion

EPR Characteristics of the Redox Components of Cytochrome bc_1 Complex. The EPR spectra of cytochromes *b*, c_1, and the ISC in the cytochrome bc_1 complex have been well characterized. In the oxidized complex, cytochromes b_L (b_{566}), b_H (b_{562}), and c_1 have peaks at $g = 3.78$, $g = 3.45$, and $g = 3.35$, respectively (41–43). The $g = 3.78$ peak of cytochrome b_L is sharp and asymmetric and difficult to power saturate even at 7 K. Peaks of cytochromes b_H and c_1 overlap to show a peak at $g = 3.4$ (Fig. 3*A*). The roughly symmetric peak ($g = 3.45$) for cytochrome b_H can be detected by using ascorbate-reduced complex. The EPR spectrum ($g = 3.35$) of cytochrome c_1 can be obtained by subtracting the ascorbate-reduced spectrum from the fully oxidized one. Because EPR spectra of cytochromes b_H and c_1 have similar power saturation behavior, they cannot be resolved by power manipulation (41–43).

The EPR spectrum of the reduced ISC of the Rieske's protein (Fig. 3*B*) shows three peaks, $g_z = 2.02$, $g_y = 1.89$, and $g_x = 1.80$ (40). While the shape and *g* value of g_x is affected by the redox states of other components (42, 43) and the presence of ubiquinone (45), the intensity of the signal of g_y ($g = 1.89$) is directly proportional to the

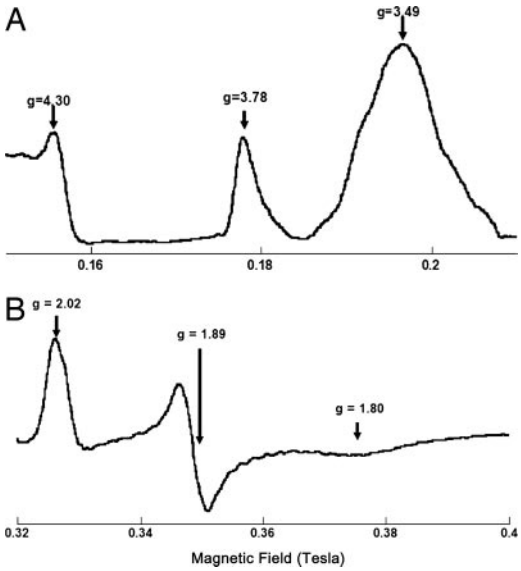

Fig. 3. EPR spectra of oxidized cytochromes *b* and c_1 (*A*) and the reduced Rieske ISP (*B*). The spectra were taken at 6 K, with the following instrument settings: microwave frequency, 9.45 GHz; modulation amplitude, 6.30 G; modulation frequency, 100 KHz; time constant, 0.655 s.

Table 1. Ubiquinol concentration-dependent reduction rate constants of cytochromes b_H and c_1

QH_2 concentration, μM	Reduction rate constants, s^{-1}	
	b_H	c_1
84	224	87
167	300	100
333	407	167
500	432	187

The cytochrome bc_1 complex was diluted in 50 mM phosphate buffer, pH 7.4, containing 1 mM EDTA and 0.01% DM to a concentration of 100 μM based on cytochrome c_1. Ubiquinol was diluted in 0.2% DM and 0.2% OG to various concentrations to give a final concentration of 1.7-, 3.34-, 6.66-, and 10-fold greater than that of cytochrome c_1. Reductions of cytochrome *b* and cytochrome c_1 were monitored by the increase of absorption at 559 nm and 550 nm, respectively, by using an Applied Photophysics stopped-flow reaction analyzer SX.18MV.

degree of reduction of ISC. Thus, the rate of ISC reduction can be followed by the $g_y = 1.89$ signal.

The EPR signature of ubisemiquinone radical is a single sharp peak at $g = 2.004$, which is easily power saturated at low temperature. Because ubisemiquinone at the Qn site is well characterized (20–24), it should not be difficult to differentiate it from any ubisemiquinone radical that is generated at the Qp site. Ubisemiquinone at the Qn site is antimycin A-sensitive and has a reduction kinetic similar to that of cytochrome b_H (37). Ubisemiquinone at the Qp site, if any, would be expected to have a kinetic similar to that of ISC or cytochrome b_L.

Presteady Reduction Rates of Cytochrome b_H and c_1 by Ubiquinol Determined by Conventional Stopped-Flow Method. The electron transfer rates between the ubiquinol and heme b_H or heme c_1 in the cytochrome bc_1 complex can be determined by mixing the fully oxidized cytochrome bc_1 complex in 50 mM Tris·HCl (pH 8.0) buffer, containing 0.33 M sucrose and 0.01% dodecyl maltoside (DM), with an equal volume of various concentrations of ubiquinol at room temperature in a stopped-flow system (SX.18MV; Applied Photophysics, Leatherhead, UK). The final concentration of cytochrome bc_1 complex is 50 μM based on cytochrome c_1, and the concentrations of ubiquinol are 84, 167, 333, and 500 μM. The substrate, ubiquinol, is prepared in the same buffer containing 0.2% DM and 0.2% octyl glucoside (OG) at double concentrations. Reductions of cytochromes b_H and c_1 are monitored by the increase of absorbance at 559 and 550 nm, respectively. Table 1 shows the observed rate constants for b_H and c_1 reduction obtained with various concentrations of ubiquinol.

Although the reduction rate constants of both cytochromes increase as the concentration of substrate increases, the degrees of increase level off as the concentration of ubiquinol approaches 500 μM. An ≈50% increase in substrate, from 333 to 500 μM, results in an increase in the rate constants for cytochromes b_H and c_1 reduction by only 6% and 12%, respectively. Because of the high hydrophobicity of ubiquinol, it is difficult to reach a final concentration >500 μM in an aqueous solution with a limited amount of detergent present. All of the subsequent rate measurements were carried out with a substrate concentration of 333 μM. Under this condition the reduction rate constants of heme b_H and heme c_1 are 403 and 164 s^{-1} with $t_{1/2}$ of 1.7 and 4.2 ms, respectively.

When the reduction of cytochromes *b* and c_1 in the stopped–flow experiment is followed with photodiode array scanning, the reduction of b_H, instead of b_L, can be clearly identified. The reaction tracings show the early reduction of heme b_H, starting before 1 ms, followed by the reduction of heme c_1 after 3 ms. The reduction of b_L is completed within the dead time of stopped-flow apparatus.

Presteady-State Reduction Rates of Cytochrome b_L and ISC by Ubiquinol Determined by Ultra-Fast Microfluidic Mixing and the Freeze-Quenching Method. The large reduction rate constant of cytochrome b_L renders the conventional stopped-flow experiment inadequate for presteady-state reduction kinetics. Also, the close absorption peaks of cytochrome b_L and b_H complicate spectroscopic rate analysis. Ultra-fast microfluidic mixing and the freeze-quenching method (44) coupled with EPR detection offers an excellent way to determine the reduction kinetics of cytochrome b_L and ISC. The ultra-fast microfluidic mixer has a dead time of 50 μs as described (44), hence it is valuable for detecting large reduction rate constants. The well resolved EPR signals of b_L and b_H make it easy to follow b_L reduction without complication from b_H.

The cytochrome bc_1 complex was diluted in the same storage buffer to a cytochrome c_1 concentration of 100 μM and mixed with an equal volume of 666 μM QH_2 in 0.2% DM and 0.2% OG in the ultra-fast microfluidic mixer (44). The reaction mixture was freeze-quenched at liquid nitrogen temperature at various time points, from 66 μs to 5 ms, packed into EPR tubes, and stored at liquid nitrogen temperature before EPR analysis.

The redox state of ISP and cytochromes *b* and c_1 were determined by EPR (42, 45) in the same sample, using a Bruker (Billeria, MA) EMX spectrometer at a temperature ≈6 K. The instrument settings were as follows: microwave frequency, 9.45 GHz; time constant, 0.655 s; and modulation frequency, 100 KHz. The modulation amplitude was 19.57 and 6.30 G for cytochromes and ISP, respectively. A microwave power of 2.15 mW was used, except for the power saturation study. During the EPR experiments it was noticed that air trapped inside the sample caused a distortion in the base line, especially in the region of magnetic field (0.15 to 0.21 Tesla) where EPR signals of b/c_1 appear. To achieve high signal sensitivity, air trapped in the sample was removed by evacuation. The freeze-quenched samples in EPR tubes were first dipped into a mixture of isopentane and liquid nitrogen. The temperature of the samples was maintained at approximately −160°C. The EPR tubes were then subjected to vacuum for 30 s before being subjected to EPR measurements. Fig. 4 shows the EPR spectra of the cytochromes *b* and c_1 (Fig. 4 *A* and *B*) and the reduced Rieske ISP (Fig. 4 *C* and *D*) at various time points after mixing with ubiquinol. The reduction of ISC was calculated from the intensity of peak to valley at $g = 1.89$ (g_y). The reduction of b_L was calculated from the integrated peak area at $g = 3.78$. Because the freeze-quenching reaction mixtures used for EPR measurements were in powder form and packed into EPR tubes in liquid nitrogen, the packing factor varied from sample to sample. To ascertain the concentration of the sample in the EPR tube at each time point, an internal spin label standard, proxyl, was added to the bc_1 sample before the rapid mixing experiment. The amounts of reduction for each redox center at various time point were normalized by using the spin label signal at $g = 1.98$. The $g = 1.98$ peak of proxyl was chosen over the two other stronger signals because it is not overlapping with the g_z signal of ISP.

As shown in Fig. 4*D*, there is no detectable semiquinone radical in the samples with a reaction time <360 μs. Semiquinone that appears after 366 μs is the radical at the O_n site, because it is sensitive to antimycin treatment and its formation rate is comparable to that of cytochrome b_H. Correlation between semiquinone formation and cytochrome b_H reduction has been reported (21).

Fig. 5 shows the reduction of ISC and heme b_L as a function of time. Note that the zero time point is based on a control sample prepared under the same conditions in the absence of QH_2. Reduction of ISC appears to be biphasic. The first phase starts at ≈100 μs and is complete within 1 ms. The reduction of heme b_L proceeds with similar kinetics but reaches a maximum at ≈400 μs. On the basis of these kinetic traces, the rate constants for electron transfer from ubiquinol to ISC and b_L at the Qp site is 2,770 s^{-1}, which is larger than the rate constants obtained by various indirect methods (36, 46, 47).

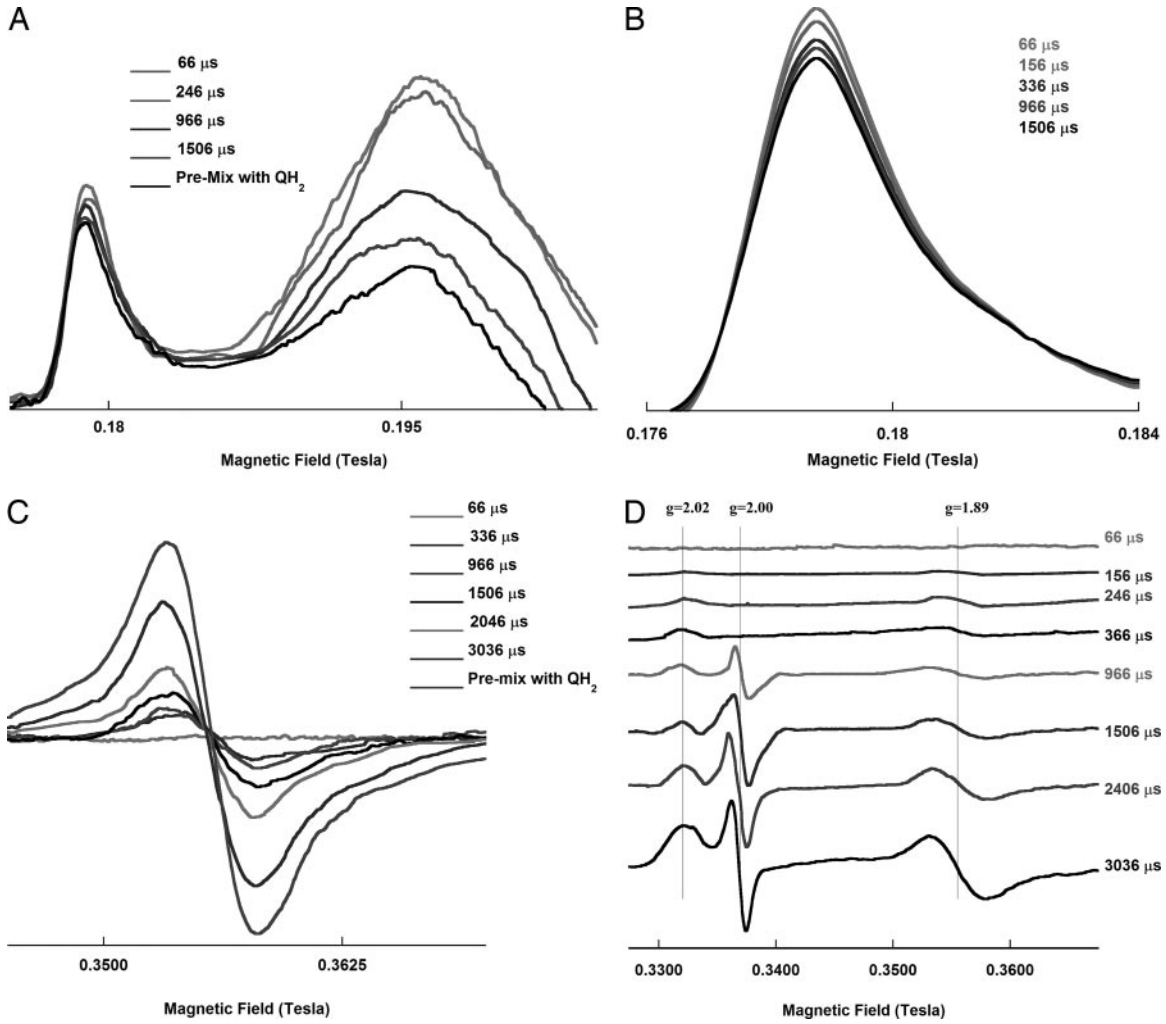

Fig. 4. EPR spectra of cytochromes *b* and c_1 and the reduced Rieske ISP at various time points after mixing with ubiquinol. The EPR spectra of cytochromes b_L and b_H/c_1 (*A* and *B*) and ISC (*C* and *D*) in the cytochrome bc_1 complex reacting with ubiquinol are shown at different time points as indicated. *B* and *C* are the EPR spectra of cytochrome b_L and ISC at $g_y = 1.89$, respectively. *D* shows the EPR spectra of ISC with $g = 2.00$ region. Samples were prepared as described in *Experimental Procedures*. The EPR spectra were taken at 6 K, with the following instrument settings: microwave frequency, 9.45 GHz; microwave power, 2.15 mW; and modulation frequency, 100 KHz; time constant, 0.655 s. The modulation amplitude used was 19.57 and 6.30 G for cytochromes and ISP, respectively. All curves are in the same order as the reaction times given.

One possibility for the biphasic reduction of ISP is the dimeric nature of the cytochrome bc_1 complex. When both monomers are in the oxidized form, the rate of reduction of ISP would be higher than that in the partially reduced complex. The slower reduction of ISP in the second phase cannot be resulted from the oxidation of ISP by cytochrome c_1 because little cytochrome c_1 is reduced in a reaction time < 2 ms. The $t_{1/2}$ for c_1 reduction was determined by conventional stopped flow to be 4.7 ms. Probably cytochrome b_L is also reduced biphasically. However, if the rate of the second (slower) phase of b_L reduction is comparable to that of b_H reduction then no increase in b_L reduction would be observed, and the kinetic would appear monophasic. In other words, the observed rate of b_L reduction is a "net" rate that includes both the reduction of b_L by ubiquinol and reoxidation by b_H. This proposal is consistent with the hypothesis of the half-of-the-sites activity of the dimeric bc_1 complex (49).

Using a light flash to initiate the electron-transfer cycle in the bacterial cytochrome bc_1 complex, a 1,650 s^{-1} rate constant was reported for electron transfer from ubiquinol to ISP at the Qp site of the complex, in a chromatophores preparation from *R. capsulatus* (46). A rate constant of 1,200 s^{-1} was reported when using a binuclear ruthenium complex to rapidly photooxidize cytochrome c_1 in the purified *R. sphaeroides* bc_1 complex (47). Using the same technique of rapid photoreduce/photooxidize cytochrome c_1 with ruthenium dimer (Ru_2D), oxidant-induced reduction of cytochrome b_H was observed with a rate constant of 250 s^{-1} in the presence of antimycin A with bovine bc_1 complex and 1,000 s^{-1} with *R. sphaeroides* bc_1 complex (48). The rate constant of the reduction of heme b_H by ubiquinol was found to be 270 s^{-1} with a photoreleasable caged ubiquinol substrate with mitochondrial cytochrome bc_1 (36).

The rate constants found in this study are significantly larger than those observed previously. The similar rate constants for electron transfer from ubiquinol to heme b_L and from ubiquinol to ISC indicate that either when the first electron of ubiquinol is transferred to the thermodynamically favored ISC the second electron is immediately transferred to heme b_L, or the two electrons of ubiquinol are transferred to ISC and b_L simultaneously from a transient ternary complex of ISP–QH_2–cytochrome *b*. Either case is consistent with the Q-cycle mechanism with no ubisemiquinone radical formation at thenQp site. The simultaneous reduction of ISC and cytochrome b_L is also consistent with the high-resolution structural data of bovine bc_1 complex.

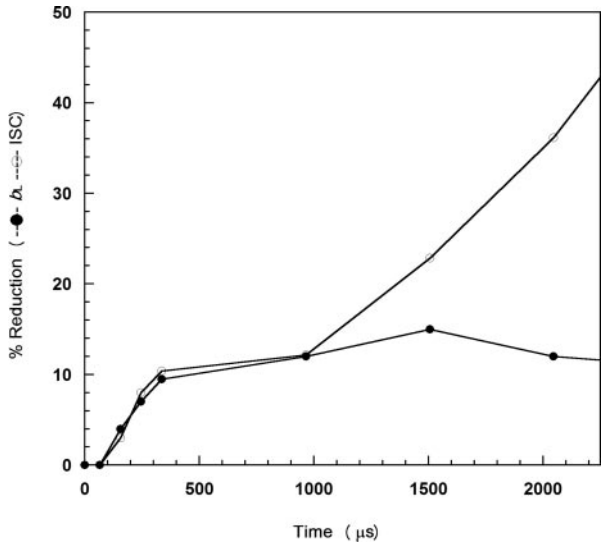

Fig. 5. The degree of reduction of ISC and heme b_L against time. ISC (○) and heme b_L (●) reduction percentage by QH_2, calculated from EPR spectra, at time points between 0 and 1 ms and 0 to 2.25 ms. The percentage reduction of b_L was calculated based on percentage decrease in the integrated area of EPR peak at 3.78 using the peak area of the fully oxidized complex as 100%. The percentage reduction of ISC was based on the signal intensity of g_y in the sample that was premixed with QH_2 as 100%.

No Ubisemiquinone Radical Is Detected at the Qp Site. If a ubisemiquinone radical is present during the oxidation of ubiquinol at the Qp site, it should be easily detected by EPR. However, there is no $g = 2.00$ signal in the EPR spectra of rapid mixed freeze-quenched samples, which shows reduction of ISP (see Fig. 4*D*) and cytochrome b_L within 500 μs of reaction time. To avoid the error of overlooking the signal of ubisemiquinone radical because of its power saturation behavior, the EPR measurements in $g = 2.00$ region were carried out at various powers. The absence of ubisemiquinone radical is consistent with the observation that the amounts of ISP reduction are equal to those of cytochrome b_L reduction in the early events of ubiquinol oxidation.

Whether or not a ubisemiquinone radical is generated at the Qp site during the oxidation of ubiquinol has been a subject of debate. It was reported that under special experimental conditions a transient antimycin A-insensitive ubisemiquinone radical was observed (50) at the Qp site. These data were later refuted (33) because the radical was found to be insensitive to Qp site inhibitors such as myxothiazol, (*E*)-β-methoxyacrylate-stilbene, or stigmatellin.

To support the idea that the first electron of ubiquinol goes to ISP and thus generates a highly reducing ubisemiquinone to reduce cytochrome b_L during the oxidation of ubiquinol at the Qp site, several plausible explanations have been offered for the failure to detect a semiquinone radical at the Qp site. One suggestion is that the radical is antiferromagnetically coupled with the reduced ISC and the radical is only separated from ISP when the second electron is transferred to b_L (34). Another suggestion is that the ubisemiquinone radical formed at the Qp site is too transient and the concentration is too low to be detected by EPR (27). The transient nature of the ubisemiquinone radical is easily understood if one pictures that the electron donor of ISP is the ubiquinol–b_L complex and not the ubiquinol alone. Once the first electron of ubiquinol in the complex is transferred to ISC, the second electron is immediately transferred to b_L, thus no ubisemiquinone radical would accumulate. It is important to note that a ubisemiquinone radical signal, $g = 2.00$, starts to accumulate when the reaction time is >500 μs. This radical is sensitive to antimycin treatment and has a formation kinetic similar to that of the reduction of cytochrome b_H, hence it is the ubisemiquinone radical of the Qn site.

Structural Basis for Concerted Bifurcated Ubiquinol Oxidation at the Qp Site. Although the information concerning the precise ubiquinol binding site in the Qp pocket is still lacking, recent structural analysis of several Qp site inhibitor-loaded crystals suggests that when ubiquinol enters the Qp pocket it arrests the head domain of ISP to the *b*-position with the formation of a transient cytochrome *b*–QH_2–ISP complex. This ternary complex is formed with the aid of hydrogen bond formation between Ser-151 and Lys-283 of cytochrome *b* and the backbone carbonyl atoms of ISP, and the formation of a hydrogen bond between the hydroxyl group at C-1 position of the substrate and the N_ε of the His-161 of ISP, a situation similar to the binding of stigmatellin. The C-4 hydroxyl group of the substrate forms a hydrogen bond with either Tyr-131 or Glu-271, a situation similar to the binding of 5-n-undecyl-6-hydroxy-4,7-dioxobenzothiazole (UHDBT) (51). If QH_2 binds in the similar position as UHDBT, the distance between the ISC and the substrate would be shorter than the distance between heme b_L and the substrate in the transient cytochrome *b*–QH_2–ISP complex. Nonetheless, in the actual cytochrome *b*–QH_2–ISP complex, the two distances could be very similar because the presence of a long alky side chain in ubiquinol may pull the ISP closer to b_L than what is observed in the *b*-position. This proposal is supported by the tighter binding of hexahydrodibenzothiophene, than UHDBT, in the yeast complex. Moreover, a water molecule might be present between ubiquinol and Glu-271 or Tyr-131, facilitating its electron transfer to b_L. Thus a comparable electron transfer rate from ubiquinol to ISC and to heme b_L could be achieved. The involvement of a water molecule in electron transfer has been observed in other systems (52). The specific role of Glu-271 in substrate binding has been questioned (53). These factors may account for the observed comparable electron transfer rates from ubiquinol to ISC and heme b_L.

Experimental Procedures

Materials. DM and OG were purchased from Anatrace (Maumee, OH). 2,3-Dimethoxy-5-methyl-6-decyl-1,4-benzoquinone bromine ($Q_0C_{10}Br$) was synthesized in our laboratory at Oklahoma State University (54). Stigmatellin, myxothiazol, and antimycin A were purchased from Sigma (St. Louis, MO). Other chemicals were of the highest purity commercially available.

Enzyme Preparations and Assays. Bovine heart mitochondrial cytochrome bc_1 complex was prepared as reported (55). The purified complex was dissolved in 50 mM Tris·HCl buffer, pH 8.0, containing 0.33 M sucrose and 0.01% DM to a cytochrome $c1$ concentration of 100 μM. In some cases, 3-maleimido-proxyl (proxyl), a spin label, was added to a final concentration of 50 μM (from a 50 mM stock solution in ethanol) as an internal standard. The mixtures were frozen at −80°C until use. The purified bc_1 complex contained 9 nmol of cytochrome *b* and 5.5 nmol of cytochrome c_1 per milligram of protein. The concentrations of cytochromes *b* and c_1 were determined spectrophotometrically by using millimolar extinction coefficients of $\Delta E_{562-575\,nm} = 28.5\ cm^{-1}\cdot mM^{-1}$ and $\Delta E_{552-540\,nm} = 17.5\ cm^{-1}\cdot mM^{-1}$ for cytochromes *b* and c_1, respectively.

For activity assay, the cytochrome bc_1 complex was diluted with 50 mM phosphate buffer, pH 7.4, containing 1 mM EDTA and 0.01% DM to a protein concentration of 0.1 mg/ml. Diluted enzyme solution (5 μl) was added to 990 μl of an assay mixture containing 50 mM phosphate buffer, pH 7.4, containing 1 mM EDTA and 100 μM cytochrome *c* in the presence or absence of inhibitor. Activity was determined by measuring the reduction of cytochrome *c* after the addition of 5 μl of 5 mM $Q_0C_{10}BrH_2$ (QH_2). A millimolar extinction coefficient of 18.5 $cm^{-1}\cdot mM^{-1}$ was used to calculate the activity. The bc_1 complex used in these experiments had a specific

activity of ≈20 μmol of cytochrome *c* reduced per minute per nanomole of cytochrome *b*.

Stopped-Flow Experiments. For the determination of electron transfer rates between the ubiquinol and heme *b* or heme c_1, the cytochrome bc_1 complex was mixed with equal volumes of various concentrations of ubiquinol at room temperature in an Applied Photophysics stopped-flow reaction analyzer SX.18MV. The cytochrome c_1 concentration of bc_1 complex was 100 μM. Ubiquinol was diluted in 0.2% DM and 0.2% OG to various concentrations. Reductions of cytochromes *b* and c_1 were monitored by the increase of absorption at 559 and 550 nm, respectively, and a photodiode array scan between 600 and 500 nm. A set of observed rate constants was measured as a function of the concentration of quinol, 1.7-, 3.34-, 6.66-, and 10-fold greater than that of the concentration of cytochrome c_1. When an inhibitor was used, the cytochrome bc_1 complex was treated with 5-fold molar excess of the inhibitor over heme c_1 for 15 min before the experiment.

Freeze-Quenching Experiments. The cytochrome bc_1 complex, with concentration of cytochrome c_1 at 100 μM, was mixed at a 1:1 ratio with 667 μM QH_2 in 0.2% DM and 0.2% OG inside the ultrafast microfluidic mixer (44) with a modification in the design of the mixing chamber (T.E., Jorge Durand, and S.-R.Y., unpublished work). The reaction mixture was freeze-quenched at various time points from 66 μs to ≈3 ms at liquid nitrogen temperature and packed into EPR tubes. All EPR tubes were stored at liquid nitrogen temperature before measurements.

EPR Experiments. The redox states of the ISP and cytochromes *b* and c_1 were determined by EPR (43), using a Bruker EMX Spectrometer at a temperature of ≈6 K. The instrument settings were as follows: microwave frequency, 9.45 GHz; microwave power, 2.15 mW; time constant, 0.655 s; and modulation frequency, 100 KHz. The modulation amplitudes used were 19.57 and 6.30 G for cytochrome and ISP, respectively. Previous experiments indicated that air trapped inside the sample causes a distorted base line, especially in the heme b/c_1 region of the EPR spectrum. To achieve high signal sensitivity, the air remaining within the sample was eliminated by first dipping the EPR tubes containing the freeze-quenched samples into a mixture of isopentane and liquid nitrogen. This solution was at a temperature of approximately −160°C. Then the EPR tubes were subjected to vacuum for 30 s before being put into the EPR spectrometer. The amount of reduction of ISP was calculated from the intensity of peak to valley around $g = 1.89$ (g_y). Reduction of b_L was calculated from the integrated peak area at $g = 3.78$. As described in *Enzyme Preparations and Assays*, spin label proxyl was added to enzyme solution as an internal standard. The data collected at each reaction time were normalized by comparison to the spin label intensity at $g = 1.98$. For detection of ubisemiquinone radical, freeze-quenching experiments were carried out with cytochrome bc_1 complex containing no proxyl internal standard.

Other Biochemical and Biophysical Techniques. Protein concentration was determined by the method of Lowry *et al.* (56). Cytochrome *b* (57) and cytochrome c_1 (58) contents were determined according to reported methods.

We thank Dr. Roger Koeppe for critical review of this manuscript. This work was supported by National Institutes of Health Grants GM30721 (to C.-A.Y.) and HL065465 (to S.-R.Y.) and Agricultural Experiment Station Projects 1819 and 2372, Oklahoma State University.

1. Trumpower BL, Gennis RB (1994) *Annu Rev Biochem* 63:675–716.
2. Berry E, Guergova-Kuras MH, Huang L-S, Crofts AR (2000) *Annu Rev Biochem* 69:1007–1077.
3. Xia D, Yu CA, Kim H, Xia JZ, Kachurin AM, Zhang L, Yu L, Deisenhofer J (1997) *Science* 277:60–66.
4. Iwata S, Lee JW, Okada K, Lee JK, Iwata M, Rasmussen B, Link TA, Ramaswamy S, Jap BK (1998) *Science* 281:64–71.
5. Zhang ZL, Huang L-S, Shulmeister VM, Chi Y-I, Kim KK, Huang L-W, Crofts AR, Berry EA, Kim S-H (1998) *Nature* 392:677–684.
6. Hunte C, Koepke J, Lange C, Robmanith T, Michel H (2000) *Structure (London)* 8:669–684.
7. Berry EA, Huang L-S, Saechao LK, Pon NG, Valkova-Valchanova M, Daldal F (2004) *Photosynth Res* 81:251–275.
8. Xiao K, Chandrasekaran A, Yu L, Yu CA (2001) *J Biol Chem* 276:46125–46131.
9. Soriano GM, Ponamarev MV, Carell CJ, Xia D, Smith J, Cramer WA (1999) *J Bioenerg Biomembr* 31:201–213.
10. Covian R, Gutierrez-Cirlos EB, Trumpower BL (2004) *J Biol Chem* 279:15040–15049.
11. Osyczka A, Moser CC, Daldal F, Dutton PL (2004) *Nature* 427:607–612.
12. Gong X, Yu L, Xia D, Yu C-A (2005) *J Biol Chem* 280:9251–9257.
13. Erecinska M, Chance B, Wilson DF, Dutton PL (1972) *Proc Natl Acad Sci USA* 69:50–56.
14. Alexandre A, Lehninger AL (1979) *J Biol Chem* 254:11555–11560.
15. Mitchell P (1976) *J Theor Biol* 62:327–367.
16. Brandt U, Trumpower B (1994) *Crit Rev Biochem Mol Biol* 29:165–197.
17. Gao X, Wen X, Esser L, Quinn B, Yu L, Yu CA, Xia D (2003) *Biochemistry* 42:9067–9080.
18. Kolling DRJ, Samoilova RI, Holland JT, Berry EA, Dikanov SA, Crofts AR (2003) *J Biol Chem* 278:39747–39754.
19. Cooley JW, Ohnishi T, Daldal F (2005) *Biochemistry* 44:10520–10532.
20. Yu CA, Nakaoka S, Yu L, King TE (1978) *Biochem Biophys Res Commun* 82:1070–1078.
21. Yu CA, Nagaoka S, Yu L, King TE (1980) *Arch Biochem Biophys* 204:59–70.
22. Ohnishi T, Trumpower BL (1980) *J Biol Chem* 255:3278–3284.
23. Esser L, Quinn B, Li F-F, Zhang M, Elberry M, Yu L, Yu CA, Xia D (2004) *J Mol Biol* 341:281–302.
24. Kim H, Xia D, Yu CA, Xia J-Z, Kachurin AM, Zhang L, Yu L, Deisenhofer J (1998) *Proc Natl Acad Sci USA* 95:8026–8033.
25. Link TA (1997) *FEBS Lett* 412:257–264.
26. Brandt U, Von Jagow G (1991) *Eur J Biochem* 196:163–170.
27. Crofts AR (2004) *Annu Rev Physiol* 66:689–733.
28. Hong SJ, Uggulava N, Guergova-Kuras M, Crofts AR (1999) *J Biol Chem* 274:33931–33944.
29. Yu CA, Wen X, Xiao K, Xia D, Yu L (2002) *Biochim Biophys Acta* 1555:65–70.
30. Kim H, Xia D, Yu CH, Xia J-Z, Kachurin AM, Zhang L, Yu L, Deisenhofer J (1998) *Proc Natl Acad Sci USA* 95:8026–8033.
31. Trumpower BL (2002) *Biochim Biophys Acta* 1555:166–173.
32. Hunte C, Palsdottir H, Trumpower BL (2003) *FEBS Lett* 545:39–46.
33. Junemann S, Heathcote P, Rich PR (1998) *J Biol Chem* 273:21603–21607.
34. Link TA (1997) *FEBS Lett* 412:257–264.
35. De Vries S, Albracht SPJ, Berden JA, Slater EC (1982) *J Biol Chem* 256:11996–11998.
36. Hansen KC, Schulz BE, Wang G, Chan SI (2000) *Biochim Biophys Acta* 1456:121–137.
37. King TE, Yu CA, Yu L, Chiang YL (1975) in *Electron Transfer Chains and Oxidative Phosphorylation*, eds Quayliariello E, Papa S, Palmieri F, Slater EC, Siliprandi N (Elsevier, New York), pp 105–118.
38. Tsai A-L, Olson JS, Palmer G (1983) *J Biol Chem* 258:2122–2125.
39. Trumpower BL, Edwards CA (1979) *J Biol Chem* 254:8697–8706.
40. Orme-Johnson NR, Hansen RE, Beinert H (1974) *Biochem Biophys Res Commun* 45:871–878.
41. Salerno JC (1984) *J Biol Chem* 259:2331–23366.
42. De Vries S, Albracht SPJ, Leeuwerk FJ (1979) *Biochim Biophys Acta* 546:316–333.
43. McCurley JP, Miki T, Yu L, Yu CA (1990) *Biochim Biophys Acta* 1020:176–186.
44. Lin Y, Gary J, Gerfen GJ, Rousseau DL, Yeh S-R (2003) *Anal Chem* 75:5381–5386.
45. Ding H, Robertson DE, Daldal F, Dutton PL (1992) *Biochemistry* 31:3144–3158.
46. Crofts AR, Wang Z (1989) *Photosynth Res* 22:69–87.
47. Sadoski RC, Engstrom G, Tian H, Zhang L, Yu L, Yu CA, Durham B, Millett F (2000) *Biochemistry* 39:4231–4236.
48. Engstrom G, Xiao K-H, Yu CA, Yu L, Durham W, Millett F (2002) *J Biol Chem* 277:31072–31078.
49. Covian R, Trumpower BL (2006) *J Biol Chem* 281:30925–30932.
50. De Vries S, Albracht SPJ, Berden JA, Slater EC (1982) *J Biol Chem* 256:11996–11998.
51. Palsdottir H, Lojero GC, Trumpower BL, Hunte C (2003) *J Biol Chem* 278:31303–31311.
52. Lin J, Balabin IA, Beratan DN (2005) *Science* 310:1311–1313.
53. Osyczka A, Zhang H, Mathe C, Rich P, Moser CC, Dutton PL (2006) *Biochemistry* 45:10492–10503.
54. Yu CA, Yu L (1982) *Biochemistry* 21:4096–4101.
55. Yu CA, Yu L (1980) *Biochim Biophys Acta* 591:409–420.
56. Lowry OH, Rosebrough NJ, Farr AL, Randall RJ (1951) *J Biol Chem* 193:265–275.
57. Berden JA, Slater EC (1970) *Biochim Biophys Acta* 216:237–249.
58. Yu CA, Yu L, King TE (1972) *J Biol Chem* 247:1012–1019.
59. Esser L, Gong X, Yang S-Q, Yu L, Yu CA, Xia D (2006) *Proc Natl Aced Sci USA* 35:13045–13050.